

19. M. K. Mitskevich, A. I. Bushik, I. A. Bakuto, et al., *Electro-Erosion Processing of Metals* (I. G. Nekrashevich, editor) [in Russian], Minsk (1988), pp. 56-57.
20. W. D. Davis and H. C. Miller, *J. Appl. Phys.*, **40**, No. 4, 2212-2221 (1969).
21. M. P. Zektser and G. A. Lyubimov, *Zh. Tekh. Fiz.*, **50**, No. 1, 78-86 (1980).
22. V. P. Afanas'ev, G. A. Dyuzhev, and S. M. Shkol'nik, "Hydrodynamic model of the plasma jet of a cathode spot of a vacuum arc" [in Russian], Leningrad (1989). (Preprint A. F. Ioffe FTI Akad. Nauk SSSR, No. 1375).
23. N. E. Perskii, V. N. Sysun, and Yu. D. Khromoi, *Teplofiz. Vys. Temp.*, **27**, 1060-1068 (1989).
24. V. P. Afanas'ev, G. A. Dyuzhev, S. M. Shkol'nik, and V. G. Yur'ev, *Proc. XIII ISDEIV*, Paris, France, 1988, pp. 220-222.
25. V. P. Afanas'ev, A. A. Logatchev, N. K. Mitrofanov, and S. M. Shkol'nik, *Proc. XIV ISDEIV*, Santa Fe, USA, 1990, pp. 187-191.
26. S. M. Shkol'nik, *IEEE Trans. Plas. Sci.*, **PS-13**, No. 5, 336-338 (1985).
27. W. H. Hayward and A. R. Wolter, *J. Appl. Phys.*, **40**, No. 7, 2911-2916 (1969).
28. G. Werner, in: *Electron and Ion Spectroscopy of Solids* (L. F. Firmens, G. Bennick, and M. Deckeiser, editors) [Russian translation], Moscow (1981), pp. 345-464.
29. G. A. Djuzhev, G. A. Lyubimov, and S. M. Shkol'nik, *IEEE Trans. Plas. Sci.*, **PS-11**, No. 1, 36-45 (1983).
30. G. A. Dyuzhev, S. M. Shkol'nik, and V. G. Yur'ev, *Zh. Tekh. Fiz.*, **48**, No. 6, 1203-1212 (1978).

INVESTIGATION OF THE THREE-DIMENSIONAL STRUCTURE OF A RF CAPACITANCE DISCHARGE

N. A. Yatsenko

UDC 537.74

The author analyzes experimental methods of investigating the three-dimensional structure of an RF capacitance discharge (RFCD), methods which would simply and reliably determine specific features, in particular: 1) the fact that near-electrode layers exists, and the degree to which processes occurring there affect the plasma discharge parameters; 2) the singularity of each RF discharge shape, weak and concentrated, and the causes and conditions for transitions between them; and 3) the mechanism for forming a discharge structure normal to the current direction, and the possibility of simultaneous ignition of both types of RF discharge in one interelectrode gap.

The RF capacitance discharge in the pressure range from tenths to hundreds of torr and frequency of the RF field from 10^6 to 10^8 Hz is one of the simplest, most reliable and efficient plasma sources in the most diverse fields: in plasma chemistry [1, 2], in plasma technology [2-4], in new laser technology [5-7], etc. Hence there is great interest in methods of obtaining, investigating and applying it.

A particularly fruitful matter for understanding the physics of the RF discharge, the mechanism by which its structure is formed, and also for the numerous applications of RFCD has been the perception of the important role of the near-electrode layers of the space discharge (NLSD) and the secondary emission processes occurring there. It was explained in [8] that there are various forms of RFCD: weak and strong, differing in the phenomena occurring in the NLSD, and for this reason there are qualitatively different spatial structures for the same external conditions: pressure and gas type, size of interelectrode gap, similarity of the RF voltages on the electrodes. For example, the discharge current density in transition from the weak discharge

form to the strong can vary by an order of magnitude and more. Here the values of the electric field, and the electron density not only vary numerically, but, which is more interesting and important for applications, their distribution in the interelectrode gap becomes qualitatively different [7, 8]. One should also note [9] that besides the equality of the number of electrons and ions incident on each electrode per period of the RF field in a steady RFCD, there is another no less important function of the NLSD, that being to stabilize the plasma column of the RFCD with the incident volt-ampere characteristic (VAC), which strictly leads also to the effect of normal current density in this kind of discharge, the dependence of normal current density on pressure p and the interelectrode gap h , and to limits of the region of existence of the weak RFCD relative to p and h .

These facts show the promise of methods of obtaining an RFCD plasma with previously assigned properties. However, to accomplish this one must have clear physical ideas about the mechanism of forming the spatial structure of each possible RFCD form, must have available reliable experimental information on their regions of existence and the causes of transition from one form of discharge to the other.

At present a number of methods are used to study the RFCD structure. In particular, the presence of NLSD in a discharge is evaluated from the constant plasma potential relative to the electrodes U_0 , which is measured by the "floating probe" method [7-18]. In fact, the excitation of constant electric fields in a discharge maintained by a sinusoidal RF field indicates that regions with nonlinear characteristics are present in these discharges, and this can be used to diagnose the spatial structure of a RFCD.

Facts indicating the presence in a steady low-pressure ($p < 1$ torr) RFCD, of constant voltage U_0 , localized between the plasma discharge and the electrodes and comparable in magnitude to the RF voltage on the electrodes U_{rf} , have long been known [10-13]. It was established that with increase of U_{rf} , the value of U_0 also increases and reaches $\approx 10^3$ V [14]. With increase of pressure U_0 decreases and for $p > 1$ torr it does not exceed a few volts [13, 15]. Regarding the dependence of U_0 on the RF supply frequency it is known that the experimental results are contradictory. According to [13] U_0 decreases with increase of frequency. In [16] an inverse dependence was observed for the same conditions.

There are several viewpoints regarding the causes of high U_0 in RFCD. One of these, considering U_0 to result from ambipolar charge diffusion [11] does not stand up to criticism [13], and is only of historical interest at present. A more fruitful idea is the explanation proposed in [13], whereby the case of high U_0 in RFCD is associated with formation of NLSD, resulting from some of the electrons leaving the discharge gap during the period of the RF field because of their higher mobility. Here it was postulated that the characteristic thickness of the NLSD d_L is determined by the amplitude of oscillation of electrons in the discharge

$$d_L = \mu_e E_m / p \omega, \quad (1)$$

where μ_e is the mobility of electrons at pressure $p = \text{torr}$; E_m is the amplitude of the RF field; and $\omega = 2\pi f$ is the field frequency. From the Poisson equation, with the condition that the ions are not mobile in the layer a formula was derived for the constant potential of an RFCD relative to the electrodes [13]

$$U_0 = 6\pi e n_p d_L^2 = 6\pi e n_p \frac{\mu_e^2 U_m^2}{\omega^2 p^2 h^2}, \quad (2)$$

where U_m is the RF voltage amplitude applied to the discharge; n_p is the density of positive NLSD ions, and it turns out that $n_p \approx n_e$; and h is the interelectrode distance.

However, the calculation using Eq. (2) does not agree with experiment. For example, with $f = 3$ MHz, $p = 1$ torr, $h = 12$ cm, $U_m = 300$ V and $n_p = 10^9 \text{ cm}^{-3}$ the value is $U_0 \approx 650$ V [13]. This calls into question the advisability of examining the oscillatory motion of plasma electrons in the RFCD [17].

The authors of [17] think that in a steady RFCD plasma, when the directed speed of electrons in the RF field is much less than their thermal speed, the concept of amplitude of oscillation of electrons in the RF field has scarcely physical meaning, and the spatial scale of separation of charge at the plasma boundary d_L is determined not by the amplitude of electron oscillations, but by the polarization length of the plasma in the electrostatic field. For small potentials ($U_0 \ll V_e$, where V_e is the electron temperature in potential units) the quantity d_L is evidently equal to the Debye radius D_e :

$$d_L = D_e = (V_e / 4\pi e n_e)^{1/2}. \quad (3)$$

For large potentials ($U_0 \gg V_e$)

$$d_L \simeq (U_0 / 4\pi e n_e)^{1/2}, \quad (4)$$

and here the fact that U_0 appears in the RFCD is treated in [17] as a result of rectifying the RF voltage in the nonlinear complex conductivity of the NLSD. For the case $p \ll 1$ torr, when we can neglect collisions of electrons in the NLSD, and consider that all the RF voltage applied to the electrodes is localized in the layers, we obtained

$$U_0 = V_e \ln \sqrt{2\pi m_e/M} - U_{rf}/\pi, \quad (5)$$

where m_e and M are the mass of the electron and ion, respectively.

However, the conclusion of the authors of [17] that the oscillatory model of spatial structure of the weak RFCD fails has not been confirmed, as indicated by the experiments of [8]. In [8] the idea was confirmed experimentally regarding the layered spatial structure of the weak RFCD, including the near-electrode regions with low active conductivity and a plasma column. Over a wide range of pressure from 1 to hundreds of torr the continuity equation for the discharge current can be written in the form

$$en_e \mu_e E_{p1}(x = h/2)/p \simeq \varepsilon \varepsilon_0 \omega E_{L1}(x = 0), \quad (6)$$

where E_{p1} , E_{L1} are the voltages of the electric field in the plasma and the NLSD. The measured value U_0 is connected with the RF voltage in the layers U_{L1} by the relation

$$U_0 = k U_{L1}, \quad (7)$$

where $k \approx 1$ is a constant.

Taking into account that the positive ion density n_p is constant to a first approximation along the discharge gap and equal to n_e in the plasma column, from the Poisson equation, taking account of Eqs. (6) and (7), we obtain an expression for the thickness of the NLSD

$$d_{L1} = k \mu_e E_{p1}/p \omega \simeq V_{dr}/\omega, \quad (8)$$

where V_{dr} is the drift speed of the electrons in the plasma.

A comparison of Eq. (8) with Eq. (1) shows that the characteristic thickness of NLSD is determined (notwithstanding [13]) by the amplitude of drift oscillations of the RFCD electrons in the plasma field E_{dr} . Here, in contrast with [13], this conclusion is not postulated, but follows uniquely from Eqs. (6) and (7). One should stress the substantial difference of Eq. (8) from Eq. (1), i.e., the fact that the electron oscillations in the derivation of Eq. (8) are assumed to occur in the electric field of the plasma column E_{p1} , and not in the "vacuum" field $E_{p1} = U_m/h$, as was assumed in [13]. It is easy to see that it is this last circumstance that leads to the strong difference (an order of magnitude) noted above of the experimental values of U_0 from those computed using Eq. (2).

An attempt to explain the observed experimental dependence of U_0 on the electrode voltage U_{rf} is unsuccessful. In fact, according to the layered model of the weak RFCD [8], $U_m \equiv U_{p1}$, but

$$U_{p1} = (E_{p1}/p) p d_{p1} \simeq (E_{p1}/p) p h, \quad (9)$$

and here d_{p1} is the length of plasma column, and when $h \gg d_{L1}$, then $d_{p1} \approx h$. Substituting Eq. (9) into Eq. (2) we can see that U_0 does not depend explicitly on the RF voltage on the electrodes nor the gas pressure, and gives close to the observed experimental value of the steady plasma potential relative to the electrodes.

In essence, U_0 is connected with U_{rf} the charged particle density $n_p \approx n_e$ and it is easy to ascertain that Eqs. (2), (6), and (9) were used:

$$U_0 = 3\pi \left(en_e \frac{\mu_e E_{p1}}{p} \right) \frac{V_{dr}}{\omega^2} = 3\pi \left(\frac{\omega}{4\pi} E_{L1} \right) \frac{d_{L1}}{\omega} \simeq \frac{3}{4} U_{L1} = \frac{3}{4} (U_{rf}^2 - U_{p1}^2)^{\frac{1}{2}}. \quad (10)$$

In the intermediate calculations of Eq. (10) the capacitance current in the NLSD is expressed in the cgs system of units, $j_L = (\omega/4\pi)E_{L1}$, and the numerical coefficient in Eq. (2) is reduced by a factor of 2, according to [19].

Thus, our analysis of the conditions for appearance of U_0 , allowing for the layered structure of the weak RFCD shows that U_0 is determined uniquely by the RF voltage on the NLSD, U_{L1} . Here the physical cause for the appearance of NLSD with high U_0 in the independent RFCD is the different mobility of the electron and ion plasma components. This circumstance unavoidably leads to the formation of an NLSD with large U_0 in a steady RFCD, which promotes equilibration of the number of electrons and ions incident on the electrodes in a period of the RF field.

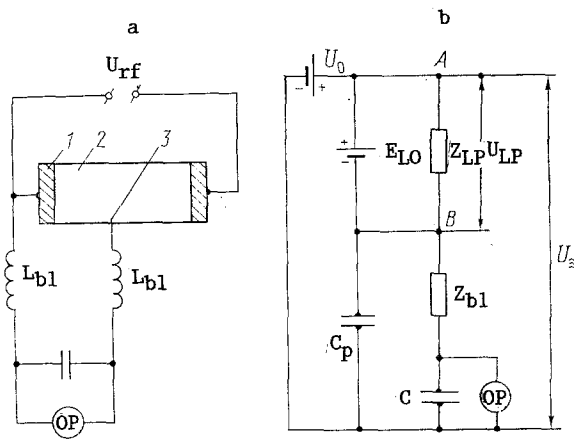


Fig. 1. Diagram in principle and the equivalent diagram for measuring the plasma constant potential: 1) electrode; 2) discharge chamber; 3) probe.

As can be seen from Eq. (10), U_0 is not explicitly connected with the pressure and the RF field frequency. However, the dependence of the RF voltage at the NLSD on p and w is given by the expression

$$U_L(p, \omega) = j_{rf}(p, \omega) V_{dr} (E_{p1}/p) / \epsilon \epsilon_0 \omega^2, \quad (11)$$

where $j_{rf}(p, \omega)$ is the discharge current density. It is known [20, 21] that with increase of p the normal, i.e., the minimum possible discharge current density increases, while E_{p1}/p , determined by the ionization balance in the plasma, and therefore by $V_{dr}(E_{dr}/p)$ varies only slightly. Therefore with increase of pressure there will be an increase of the minimum possible value of U_{Lmin} for which a weak RFCD can exist, and according to Eq. (7) U_0 will increase, which contradicts the conclusions of [13]. But this contradiction is removed if we consider the actual RFCD structure, and, as was already noted, by U_m in Eq. (2) we mean the RF voltage in the plasma and not only the electrodes.

Thus, considering the positive ions to be motionless, from the condition that a weak RFCD be steady it follows that U_0 is equal to the amplitude U_L applied to the NLSD, independently of pressure to an accuracy up to the electron temperature. Allowance for the actual motion of the ions in the layer cannot reduce this value considerably, since $\mu_e/\mu_p > 10^2$. However, probe measurements of an RF plasma at constant potential [13, 15] indicate a sharp fall of U_0 with increase of pressure $p > 1$ torr.

We now consider in detail a method of probe measurements in RFCD. One was given in [18]. The essence of the method is that for correct measurements of U_0 in an RF discharge it is necessary and sufficient to organize the measurements such that the RF component of the voltage between the probe and the plasma U_{LP} be small. To this end it is proposed to include a throttle between the probe and the measuring scheme, the throttle having a large inductance for the RF current. A similar method was used also in [13, 15]. A schematic is shown in Fig. 1a, and an equivalent diagram in Fig. 1b where the following notation is used: U_{∞} is the RF voltage between the region of unperturbed plasma where the probe is located (point A) and the ground; U_0 is the constant voltage between the plasma and the electrode; E_{L0} is the constant voltage between the plasma and the probe surface; C_p is the parasitic capacitance of the probe and the blocking element to ground, and Z_{b1} is the impedance of the probe blocking element for the RF voltage; Z_{LP} is the impedance of the plasma-probe layer; C is the capacitance of the condenser to which U_{OP} is applied, the constant voltage recorded; L_{b1} is the inductance blocking the RF current; and U_{LP} is the RF voltage in the near-probe layer.

It follows from Fig. 1b that

$$U_{OP} = U_0 - E_{L0}. \quad (12)$$

According to Eq. (12), the method error in measuring U_0 is linked to E_{L0} . We write E_{L0} as the sum of two independent terms: $k_1 V_e$, which depends on the plasma electron temperature, and $k_2 U_{LP}$ the component due to flow of RF current to the probe (k_1 and k_2 are constants). The term $k_1 V_e$ is defined by the plasma properties, and it cannot be removed if the probe is located in the plasma. The second term is a linear function of U_{LP} . It would seem that by choosing Z_{b1} we can lower $k_2 U_{LP}$ to a value comparable with $k_1 V_e$. However, the presence of the parasitic capacitance and the blocking element C_p relative to ground makes

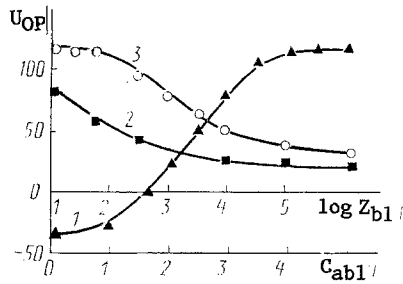


Fig. 2

Fig. 2. Dependence of probe readings on the value of the blocking element Z_{bl} (1), and on the additional capacitance (2, 3); 2) blocking element in the form of a throttle; 1, 3) in the form of a low-capacitance high-ohm resistor. A weak RFCD in air at $p = 10$ torr, $f = 13.6$ MHz, $h = 30$ mm; the probe is at the center of the discharge gap. U_{OP} is in V; C_{abl} in pF.

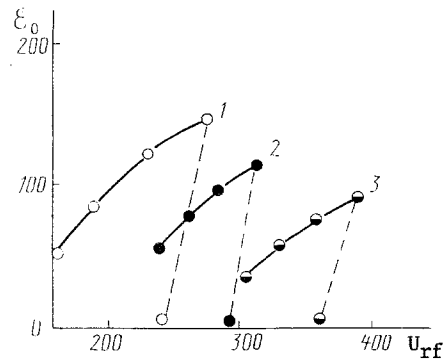


Fig. 3

Fig. 3. Typical dependences of the constant emf (in V) on the RF voltage on the electrodes \mathcal{E}_0 (V) in a coaxial electrode system.

it meaningless to increase the blocking element above $Z_{bl} > 1/(\omega C_p)$ because of the shunting action of C_p . Therefore, the only way to increase the accuracy of measurement of U_0 is associated with a decrease of C_p , which reduces to a rational location of the probe and the blocking element, the choice of their size, etc.

An additional difficulty in evaluating the measurement accuracy of U_0 is the absence of reliable theoretical models that would allow evaluation of Z_L at average and high pressures. The technique suggested in [22] for a theoretical estimate of the probe measurement error is valid only for low pressures in the discharge ($p \ll 1$ torr), when the near-probe layers of space charge can be considered collisionless. For other conditions an experimental check of correctness of probe measurements of U_0 becomes important.

It was shown above that the U_0 measurement accuracy is mainly influenced by the value of U_{LP} , which must satisfy the inequality $U_{LP}/U_\infty \ll 1$. According to Fig. 1b this is equivalent to satisfying the condition

$$|Z_{LP}|/|Z_\Sigma| \ll 1. \quad (13)$$

Here Z_Σ is the impedance of parallel combinations of C_p and Z_{bl} . Here the capacitance C is not computed, since its value may always be chosen to satisfy the condition $1/(\omega C) \ll Z_{bl}$.

We can check experimentally the validity of the above ideas on accuracy of probe measurements of U_0 by monitoring the variation of Z_{bl} and C_p . Figure 2 shows the test results. Curve 1 shows the dependence of U_{OP} on Z_{bl} on a semilogarithmic scale, and curves 2 and 3 show the dependence of U_{OP} on C_p , measured by additional switching of the capacitance C_{abl} .

For small Z_{bl} the probe potential is negative. Then near the probe one sees optical effects similar to the near-electrode effects, i.e., for small Z_{bl} the probe is itself a supplementary electrode. The dependence of U_{LP} on Z_{bl} at first increases monotonically, and then becomes saturated. This result confirms the correctness of the equivalent scheme (Fig. 1b), but allows no comment on the accuracy of measurements, since the cause of saturation of the dependence $U_{OP}(Z_{bl})$ remains an open question. The latter can occur in two cases: either U_0 is fixed and indeed draws near to U_0 , or the shunt action of C_p limits the increase of the effective blocking impedance Z_Σ .

The situation becomes clear when one analyzes the behavior of curves 2 and 3 of Fig. 2. If saturation of U_{OP} appears when the artificially inserted parasitic capacitance is reduced to zero, then the error of measurement by the probe and in the given conditions is close to a minimum, determined only by the correction to the plasma electron temperature T_e . In particular, it follows from Fig. 2 that when a low-capacitance resistor is used as Z_{bl} the measurement accuracy of U_0 increases substantially, and one sees saturation of U_{OP} reached for $C_{abl} \rightarrow 0$, which cannot be said about curve 2. This is evidently connected with the large parasitic capacitance of the throttle, since the probes themselves were the same in both cases.

We note that the observation of large $U_0 \gg T_e/e$ in the entire region of existence of RFCD [7, 8] indicates only the presence of RFCD NLSD in the spatial structure, but says nothing about their thicknesses. However, if we measure the distribution of $U_0(x)$ along the current direction we can determine the characteristic thicknesses of NLSD d_L and evaluate the constant electric field at each section of the layer [7, 8, 23].

One should stress especially that the accuracy of measuring U_0 is influenced appreciably by the dependence of Z_{LP} on the external conditions under which the tests are conducted: the type and pressure of gas, the frequency of the RF field, etc. An example of this are the results of probe measurements of U_0 in [13, 15]. Experiments conducted with the same probe, i.e., for $Z_{bl} = \text{const}$ nevertheless do not allow one to fix high values of U_0 for $p > 1$ torr, while for pressure $p \ll 1$ torr the same probe gave satisfactory results in agreement with data measured by other methods (e.g., based on the measured energy of positive ions emerging from the NLSD of RFCD [13]). Evidently, with increase of pressure in the discharge chamber the value of Z_{LP} also increases, and the ratio Z_{LP}/Z_Σ appearing in Eq. (13) decreases along with the measurement accuracy. The steps taken in [8] led in essence to an increase of Z_Σ which enabled the probe method to observe high values of U_0 in RFCD for $p \gg 1$ torr (in contrast with [13, 15]).

An effective method of showing the occurrence of high U_0 in an RFCD is to record and analyze the behavior of the constant emf \mathcal{E}_0 arising between the electrodes of an asymmetrical RF capacitance discharge at average and high pressure [24]. We shall consider this method. It was shown above that U_0 is determined by the RF voltage on NLSD, Eq. (7). But U_L in turn is a function of j_{rf} and the effective impedance of the NLSD, reduced to unit area, is Z_L ($U_L = j_{rf}Z_L$). Here

$$Z_L = 1/(\omega C_L + 1/R_L), \quad (14)$$

where R_L , $C_L = \varepsilon\varepsilon_0/d_L$ are the effective values of the active resistance and the capacitance of the PSPZ of unit area, $\varepsilon_0 = 8.85 \cdot 10^{-14}$ F/cm, and $\varepsilon = 1$ is the dielectric permeability.

In a weak RFCD $\omega C_L \gg 1/R_L$ [21], and d_L is practically independent of j_{rf} [9]. Therefore $U_0 \sim j_{rf}$. Thus, if the RFCD burns steadily in conditions where the RF current density in one of the NLSD j_1 is greater than the value j_2 in the other near-electrode layer, then $U_{01} > U_{02}$, i.e., between the electrodes of an asymmetrical RF discharge there is a constant emf \mathcal{E}_0 :

$$\mathcal{E}_0 = U_{01} - U_{02}. \quad (15)$$

Technically it is very simple to set up an asymmetrical RFCD in a coaxial electrode system. In such an electrode configuration filled with plasma of a low-pressure RFCD ($p \ll 1$ torr) the battery effect has indeed been observed, i.e., the appearance of high \mathcal{E}_0 and constant currents I_0 when one closes a circuit containing \mathcal{E}_0 [25]. Since in low pressure regions the existence of NLSD, the cause of the appearance of large U_0 , has been rigorously established by different methods, the appearance of \mathcal{E}_0 in the above conditions is admissible.

The position is different in the region $p > 1$ torr, where the situation is not unique and there are test data [13, 15] indicating a sharp reduction of U_0 with increase of p . Therefore it is appropriate to use the battery effect for an independent check of the existence of NLSD and large U_0 in RFCD for $p > 1$ torr.

Figure 3 shows typical dependences $\mathcal{E}_0(U_{rf})$ [24], obtained in a coaxial electrode system. Curves 1 and 2 were taken in an RF discharge in air with $p = 7.5$ and 15 torr, respectively, and curve 3 was taken in helium at $p = 100$ torr. The discharge was excited at frequency $f = 13.6$ MHz. The constant potential of the smaller electrode was negative relative to the larger electrode.

We call attention to two special features in the behavior of $\mathcal{E}_0(U_{rf})$: the high values of \mathcal{E}_0 for large $p \gg 1$ torr and the sharp decrease of \mathcal{E}_0 (practically to zero) when an RF voltage on the electrodes of some value U_{per} is reached, the value depending on the kind of gas, the pressure and the electrode material.

Analysis of the results leads to a unique conclusion: independently of the pressure in an RFCD NLSD are formed, the constant voltage on which reaches hundreds of volts. The decrease of \mathcal{E}_0 when the value of U_{per} exceeds the RF voltage on the electrodes does not mean that the NLSD vanishes, but points to the appearance in the interelectrode gap of a qualitatively different strong RFCD regime [8], when $U_{01} = U_{02}$ (in spite of asymmetry of the electrodes).

In fact, for $U_{rf} \geq U_{per}$ there is breakdown of the NLSD of the RFCD, and a qualitatively new spatial structure is formed in the interelectrode gap, a structure in which the RF voltage on each of the NLSD, U_{L1} and U_{L2} are determined (like the cathode region of the normal glow discharge) only by the nature of the gas and the electrode material [8]. But since the gas filling the interelectrode gap is the same, and the electrodes are made of one material, then $U_{L1} = U_{L2}$ in each ignition regime. Hence it follows, taking account of Eq. (7), that $U_{01} = U_{02}$ and, according to Eq. (15) $\mathcal{E}_0 = 0$.

When the negative glow discharge completely fills the electrode with the smaller area one observes a nonzero value of \mathcal{E}_0 , since in this case the electrode of smaller area functioned in an anomalous regime, i.e., as a larger U_L .

An additional experimental check was performed of the ideas concerning the cause of the sharp decrease of \mathcal{E}_0 in the above experiments with transition of the RFCD to a strong regime. An RF discharge was excited in a symmetrical electrode system ($S_1 = S_2$), but one of the electrodes was made of copper, and one of duralumin. It was observed that in the weak form of RFCD, i.e., when the NLSD was not pierced, the value of \mathcal{E}_0 was close to zero for all values of U_{rf} in the range $U_{z1} \leq U_{rf} < U_{per}$ (U_{z1} is the minimum RF voltage on the electrodes for which there exists a weak form of RFCD in the given specific conditions). However, upon transition to a strong burning regime $\mathcal{E}_0 \neq 0$. For example, for a strong RFCD in air $\mathcal{E}_0 = 70$ V, and the copper electrode had the smaller potential.

Thus, analysis of the measured \mathcal{E}_0 not only shows the appearance in RFCD of high U_0 independently of the pressure, but also allows conclusions to be drawn as to the form of existence of the RFCD (weak or strong). The possibilities of the method are substantially expanded if a constant current I_0 , excited by \mathcal{E}_0 , flows between the RF electrodes (e.g., one can find the active conductance of the discharge, explore its internal structure by joining the RF electrodes via a throttle, etc).

The distribution of constant plasma potential in the interelectrode gap can be used also to study the structure of the RFCD transverse to the RF current direction. This problem can be solved with the aid of the unperturbed RF discharge technique [7]. According to [7] one of the RF electrodes is sectioned relative to the constant field component, but is provided with the same potential of all the sections of RF components, e.g., by switching each section of the electrode to a grounded metal plate via a separate high-value capacitance. In particular, the sectioned electrode can be made in the form of a circular disk constructed from mutually insulated metal rings. The experiment shows that the RFCD in this case does not differ in its optical and electrical characteristics from one burning between continuous electrodes. However, when one uses the sectioned electrode it is possible to measure U_0 not only between the plasma and the electrodes (see above) but also between any two rings $V_0(m, n)$ (where m and n are ring numbers), and from the magnitude of $V_0(m, n)$ for the different m and n one can evaluate the degree of radial nonuniformity of the discharge.

The mechanism for relating $V_0(m, n)$ with radial nonuniformities is the following. When the RFCD is uniform in the radial direction, then d_L and j_L do not depend on the radius. Hence it follows that U_0 is also independent of the radial coordinate (since $U_L \sim j_L d_L$), while $U_0 \sim U_L$, i.e., $V_0(m, n) = U_0(m) - U_0(n)$. In the contrary case $V_0(m, n) \neq 0$ and the degree of radial nonuniformity of the discharge is determined.

This method can be used also to study the distribution of RF current over the electrode surface. It has been used to investigate the phenomenon, interesting and important for applications, of simultaneous co-existence of weak and strong forms of RFCD in a single interelectrode gap [26].

The constant electric current method of probing an RFCD [8, 21] gives good information on the RFCD structure and is simple to accomplish; combined with calorimetric measurements of power dissipated in the discharge it gives a unique evaluation of the burning regime, determines the integral characteristics of the NLSD and the plasma: thickness of layers, the ohmic resistances R_L, R_p , the electric field intensity in the plasma E_{pl} , etc.

The essence of the method is that a constant current source with controlled output voltage U_p is switched to the RF electrodes, if they are not covered with dielectric, or to additional electrodes inserted in the discharge gap if the primary electrodes are covered; then the volt-ampere characteristics of the circuit are taken, including the RFCD being measured. From the linear section of the volt-ampere characteristics of the probing circuit one can find the active conductance of the object located between the probing electrodes. If one must exclude from consideration the layers between the additional electrodes the volt-ampere characteristics of the probing circuit are taken for different distances between the additional electrodes.

The attraction of the constant electric current and active probe method for the RF discharge is the simplicity of separating the discharge current I_{rf} and the probing current I_p by using frequency-dependent elements (induction coils and capacitors).

We shall assess the method of determining d_L, R_L in both burning regimes of the RFCD using active probing. In this case it is desirable to use planar cooled electrodes of area S , not coated with dielectric, and vary the distance h between them. Since the problem is to determine the integral characteristics of the NLSD, to eliminate the influence of the plasma column on the measured results, we choose h as the minimum for which the required burning regime is obtained.

To accomplish the method requires measurement of the RF voltage on the electrodes U_{rf} , the discharge current I_{rf} , and simultaneously to record the area of the electrodes S_{pl} occupied by the discharge. The RF oscillator is switched to the electrodes via the capacitance C_{bl} . To the same electrodes, via the blocking throttle L_{bl} we switch a stabilized constant voltage source with controlled U_p and current measuring device I_p . Due to the presence of L_{bl} and C_{bl} , the RF discharge current and the constant

probing current are completely separated here. The quantity I_{rf} is determined by U_{rf} and the total impedance of the discharge gap, while I_p depends on U_p and the active conductance of the discharge. By choosing h the influence of the plasma column of the RFCD on the conductance of the discharge gap can be minimized. Then the expression $U_p S_{pl}/I_p$ determines the active resistance of the near-electrode region R_L per unit area, while $U_{rf} S_{pl}/I_{rf}$ gives the total impedance of the same layers Z_L , also referenced to unit area.

Knowing R_L and Z_L we compute the effective capacitive component of conductance of the layers and therefore we compute the thickness d_L of the near-electrode layers, averaged over the period of the RF field, in different burning regimes, and establish its dependence on the gas pressure and the frequency, taking the above measurements for different p and w . Under the hypothesis that the NLSD with average over a period of the RF field can be represented as a planar capacitance with leakage R_L , it is not difficult to obtain an expression linking the effective value of d_L with the experimentally measured quantities:

$$d_L = \varepsilon \varepsilon_0 \omega / (1/Z_L^2 - 1/R_L^2)^{1/2}. \quad (16)$$

The validity of identifying the value of d_L from Eq. (16) with the actual thickness of the near-electrode layers of spatial charge follows from the observed structure of the RFCD in the experiment [8] and from the fact that the recorded form of $U_{rf}(t)$ and I_{rf} is close to sinusoidal. This points to the linearity of the circuit as a whole, in spite of the nonlinear characteristics of each layer, as indicated by the occurrence of U_0 in the (see above). Thus, although the thickness of each of the layers $d_{L1}(t)$, $d_{L2}(t)$ oscillates with time, the total value $d_{L1}(t) + d_{L2}(t) = \text{const}$.

In considering method errors of the measured results one must take account of the specifics of each of the RFCD forms appearing in each case, that the NLSD of the strong RFCD as well as the cathode region of the constant current glow discharge, independent of the plasma column. By reducing h we can set up conditions where $U_{rf} = U_L$. In the weak discharge the main source of positive ions for the NLSD is the plasma column, which leads to an error in determining d_L from Eq. (16) (overestimate), since U_{rf} in the weak RFCD always exceeds U_L , because of the presence of the RF voltage in the plasma column. Monitoring of the excess of U_{rf} with respect to U_L is accomplished by measuring the phase shift φ between U_{rf} and I_{rf} . It is not difficult to show, taking into account the layered structure of the RFCD, that for $\varphi > \pi/3$ the relative overestimate $(|U_{rf}| - |U_L|)/|U_L| < 0.15$.

One more source of error in determining j_{rf} and d_L in the weak discharge appears in measuring I_{rf} , when due to small h (in the partially filled plasma of the interelectrode gap in the direction normal to the current) the shunting influence of the RF current flowing outside the plasma discharge becomes important. This influence can be reduced to a minimum by increasing I_{rf} to a level where the discharge fills the entire interelectrode gap.

Measurements in the constant current probing circuit also have their special features. The expression $R_L = U_p S_{pl}/I_p$ is correct when the following conditions pertain: 1) the passage of I_p through the discharge gap does not influence the structure of the NLSD; 2) in the process of RFCD burning a constant emf \mathcal{E}_0 does not arise between the electrodes, i.e., the discharge is a passive load for the source U_p . Experiment shows that both conditions can be violated in practice. For large U_p the volt-ampere characteristics of the probe circuit become nonlinear, which indicates that the probe voltage is affecting the NLSD structure, especially in the weak burning regime. A decrease of $U_p < 5$ V represents more rigid requirements regarding suppression of RF pickup in the measuring circuits. It proves practically impossible to fulfill the second condition, since even for $U_p = 0$ the current I_p in the strong regime reaches several milliamperes, which generates an \mathcal{E}_0 value of several volts between the RF electrodes. To eliminate method error in this case I_p must be measured twice: for $U_p \neq 0$ and $U_p = 0$, and depending on the direction of the currents then recorded the true value of I_p is taken from the sum, if the currents are directed counter to each other, or from the difference, if the currents are parallel.

We turn now to an experimental proof of the existence of the normal current density effect in both forms of RFCD. The direct method, based on measuring the cross sectional area of the discharge for different currents, is often very laborious, since the outlines of the near-electrode layers, especially in the strong discharge, are far from the correct geometrical form, and may move continuously, in addition, over the electrode surface. Therefore it is appropriate to use the active RFCD probe method considered above, or more exactly, the dependence of R_L on the parameter $1/I_{rf}$. Typical results obtained in the strong RFCD at frequency 13.6 MHz show that to good accuracy the experimental points fall on straight lines satisfying the condition $R_a = A_0/I_{rf}$, where A_0 is a constant determined by the type of gas and the electrode material (practically did not vary for each series of tests). This gives a basis to postulate that the specific characteristics of the discharge also do not vary with increase of I_{rf} , and the results obtained are a consequence of the linear dependence of S_{pl} on I_{rf} , i.e., in the strong RFCD, when it does not fill the

entire electrode area, the quantities j_{rf} , U_L , d_L do not depend on I_{rf} . This technique can be applied if $I_{rf} \gg I_n$ (I_n is the RF current passing outside the discharge). In the contrary case one must take account of I_n .

We shall now apply the method of active probing of an RFCD in a direction normal to the RF current. In this case the basic electrodes (RF) are covered with dielectric, and the additional electrodes are located in the interelectrode gap. Here the additional electrodes can be achieved by moving the RF electrodes along the surface, or their number can be more than two.

Let l_{12} be the distance between the 1st and 2nd electrodes, and l_{23} between the 2nd and 3rd electrodes, where $\Delta l = l_{12} - l_{23} \neq 0$. It is clear that for the same probe current I_p , chosen in the linear sections of the volt-ampere characteristics of both probe circuits, we can write:

$$\begin{aligned} U_{p12} &= (R_{L1} + R_{L2}) I + \frac{l_{12} I_p}{\sigma_{\perp} S_{\perp}}, \\ U_{p23} &= (R_{L2} + R_{L3}) I + \frac{l_{23} I_p}{\sigma_{\perp} S_{\perp}}. \end{aligned} \quad (17)$$

Here R_{L1} are the active resistances of the near-electrode regions of the additional electrodes, where electrodes 1 and 3 can move in such a way that $R_{L1} = R_{L3}$; S_{\perp} is the cross sectional area of the plasma through which the current I_p flows; σ_{\perp} is the conductance of the RF discharge with the probe in the direction normal to the RF current.

From Eq. (17), allowing for $R_{L1} = R_{L3}$ it follows that:

$$\sigma_{\perp} = I \Delta l / S_{\perp} (U_{p12} - U_{p23}). \quad (18)$$

Comparison of σ_{\perp} with the active-conductance of the weak RFCD obtained when probing along the RF current and σ_{\parallel} in the same conditions shows that $\sigma_{\perp} / \sigma_{\parallel} > 10^2 - 10^3$, which points once again to the layered structure of the weak RFCD, including capacitive NLSD and a plasma column joined in series, where $\sigma_L \ll \sigma_{pl}$.

We now consider application of the method of active probing of the RFCD with a constant electric current to determine the plasma column parameters, and also for an added check of the data obtained above on the spatial structure of the RF capacitive discharge. Both these questions are of fundamental importance in understanding the physics of the RFCD. The fact is that although the variation of impedance of the interelectrode gap when a discharge is present was known long ago [27], and there are contemporary investigations of this effect [28, 29], nevertheless the status is unsatisfactory [29, p. 63].

In [29] the valid comment was made that according to the data on modeling the actual RF discharge [28], the appearance of a plasma in the interelectrode gap brings added capacitance C_s to the supply circuit, the value in general depending on the frequency of the excited field and on the power applied to the plasma P_{pl} (more accurately, on the pulse shape of the RFCD). Here the conclusion is drawn that this capacitance C_s appears to increase the capacitance of the empty interelectrode gap C_0 . According to the authors of [29], this "indicates the parallel nature of their combination". It can be seen that the latter statement is not unique. It is entirely permissible that the increase of capacitance of the interelectrode gap ΔC when an RFCD burns in it can be due to the decrease of the "effective" distance between the electrodes, these being coatings of the empty capacitance C_0 from the value h in the absence of plasma to $2d_L = h - d_{pl}$ when a plasma column is excited with dimension d_{pl} along the current.

In this case the increase of capacitance of the interelectrode gap when the RF discharge arises can be evaluated from the expression

$$\Delta C = C_0 (h - 2d_L) / 2d_L. \quad (19)$$

In deriving Eq. (19) it was assumed that the parasitic capacitance of the electrodes relative to the surrounding space C_{par} does not change when the discharge is burning and that the capacitance of the plasma column can be neglected.

Thus, the experimentally observed increase of capacitance of the interelectrode gap when a discharge is burning can be interpreted otherwise than in [29]. The scheme of moving the RFCD to achieve $\Delta C > 0$ represents a series $R_{pl} C_L$ circuit, and not a parallel one, as suggested in [29]. But when the question arises of interpreting the ohmic resistance of the RF capacitive discharge R_a , which is introduced in [27, 29], and identified as the ohmic resistance of the plasma. To elucidate this question in our study we proposed an improved method of probing the RFCD with a constant electric current, enabling us to draw unique conclusions as to the spatial structure of the RF capacitive discharge.

The modification comprises the fact that the method examined above is supplemented by one more element, the possible monitoring of the change of the interelectrode gap h to the high accuracy of ± 0.1 mm. The implementation takes the form of measuring the ohmic resistance of a discharge of unit area r (as described above) as a function of the interelectrode gap h , i.e.,

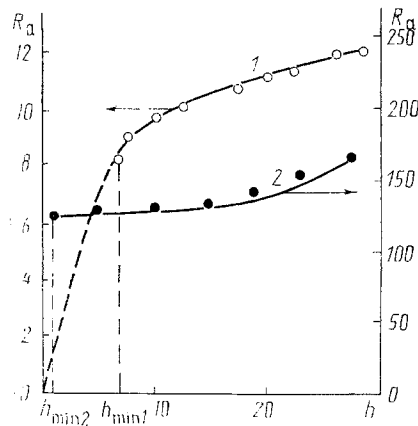


Fig. 4. Measured active resistance of RFCD R_a for various values of the interelectrode gap h (mm). Discharge in air at $p = 10$ torr, $f = 13.6$ MHz: 1) $R_a(h)$ in a weak discharge (k Ω); 2) in a strong discharge (Ω); $h_{\min 1}$, $h_{\min 2}$ are the minimum values of h for which one can excite the weak or strong form of the RFCD, respectively, in the given conditions.

$r = r(h)$. Here the gas temperature T and the discharge current density j_{rf} are kept constant. Special attention was paid to fulfilling the last condition, since j_{rf} depends on h , other conditions being equal [21].

For unchanged T and j_{rf} we can consider that the layer parameters, including their active resistance R_L did not change during the experiment. Then a valid expression for r as a function of h is:

$$r(h) = R_L + R_{p1} = R_L + (h - 2d_L)/\sigma_{p1}. \quad (20)$$

If we follow the discharge model examined in [29], then $r = h/\sigma_{p1}$. Analysis of typical experimental dependences $R_a(h)$ (Fig. 4) shows the validity of the layer model of the RFCD, including the NLSD and the discharge plasma column, which can be modeled as a series $R_{p1}C_L$ circuit.

Further, with the proposed method one can determine the conductance of the plasma column. In fact, from Eq. (20) it can be seen that

$$\sigma_{p1} = \frac{dh}{dr}. \quad (21)$$

Among the other methods of investigating the spatial structure of the RFCD we should single out optical methods [8, 15, 30], and particularly those [15, 30] which focus on fluctuations of luminosity of the RFCD at the basic RF field frequency, since this effect is due to the presence of near-electrode layers in the RFCD structure.

The methods described here of investigating the spatial structure of the RFCD are applicable not only for constructing an adequate test of the physical model of the steady RF capacitive discharge. They are necessary for developing and optimizing the parameters of a new generation of quantum electronics instruments – slotted gas lasers [6, 7, 31, 32]. In fact, as can be seen from Fig. 4, the active conductance of the NLSD, its thickness and other discharge parameters depend on the RFCD burning regime (weak or strong [8]). It has been shown that in the development of the slotted gas laser on molecular or atomic transitions the weak RFCD is preferred, while for the creation of ion slotted lasers the strong regime is an advantage [6, 7, 32]. The specific data on the discharge required to build lasers can be obtained using the techniques examined above.

Information on the constant potential of the RFCD plasma U_0 is extremely important in plasma technology, since U_0 determines the energy of the ion beam bombarding the surface being processed.

One can find interesting applications also for the battery effect, since the constant emf between the electrodes of an asymmetrical RFCD depends on the composition of the gas, i.e., this phenomenon can be used for express analysis of composition of a gas in a discharge chamber, a gas laser, for example.

NOTATION

U_0 , constant potential of the RF discharge plasma relative to the electrode; U_{rf} , I_{rf} , j_{rf} , RF voltage on the electrodes, RF current and its density; p , gas pressure; h , interelectrode gap, d_L , thickness of the NLSD; μ_e , μ_p , mobility of electrons and ions in the plasma; e , m_e , V_{dr} charge, mass, and drift velocity of electrons in the plasma; M ion mass; T_e electron temperature of the plasma, including also potential units V_e ; E_{pj} , E_L , intensity of the RF field in the plasma and the NLSD; U_{∞} , U_{LP} amplitude of the RF field; E_{L0} RF voltage between regions of the unperturbed plasma containing a probe, and the ground, probe and RFCD plasma, respectively; E_{L0} constant voltage between the plasma and the probe surface; ϵ_0 , ϵ dielectric constant and permeability, respectively; C_p parasitic capacitance of the probe relative to ground; Z_{bl} , Z_{LP} impedance of the probe blocking element and the near-probe layer; Z_{Σ} impedance of a parallel combination of C_p and Z_{bl} ; U_{OP} recorded constant voltage in the probe circuit; C_{bl} , L_{bl} blocking elements; \mathcal{E}_0 constant emf between the electrodes of an asymmetrical RFCD; S , S_{pl} area of the working surface of the electrode, and area of the electrode filled with the plasma; $V_0(m, n)$ constant difference of potentials between elements of a sectioned electrode with numbers m and n ; U_p , I_p probe voltage and current; R_L , R_{pl} , r ohmic resistance of the NLSD, RFCD plasma and of the entire discharge as a whole, referenced to unit area; C_L , Z_L effective capacitance and impedance of the NLSD of unit area; φ phase shift between I_{rf} and U_{rf} ; σ_p , σ_{\perp} active conductance of the RFCD when probed along the current direction and in the transverse direction; l_{ij} distance between auxiliary electrodes i and j ; C_0 , C_s capacitance of the interelectrode gap, empty and filled with plasma; R_a , σ_{pl} active resistance and conductance of the RFCD plasma.

LITERATURE CITED

1. V. D. Rusanov and A. A. Fridman, Physics of the Chemically Active Plasma [in Russian], Moscow (1984).
2. IEEE Trans. Plasma Sci. (Special Issue on Physics of RF Discharges for Plasma Processing), **PS-14**, No. 2, 7-197 (1986).
3. B. S. Danilin and V. Yu. Kireev, Use of Low-Temperature Plasma for Etching and Cleaning Materials [in Russian], Moscow (1987).
4. B. S. Danilin, Use of Low-Temperature Plasma for Depositing Thin Films [in Russian], Moscow (1989).
5. V. I. Myshenkov and N. A. Yatsenko, Kvantovaya Élektron., **8**, No. 10, 2121-2129 (1981).
6. N. A. Yatsenko, Gas Lasers with High-Frequency Excitation [in Russian], Moscow (1989) (Preprint/IPM Akad. Nauk SSSR, No. 381).
7. N. A. Yatsenko, Spatial Structure of the High-Frequency Capacitative Discharge and Prospects of Its Use in Laser Technology [in Russian], Moscow (1988) (Preprint/IPM Akad. Nauk SSSR, No. 338).
8. N. A. Yatsenko, Zh. Teor. Fiz., **51**, No. 6, 1195-1204 (1981).
9. N. A. Yatsenko, Zh. Teor. Fiz., **58**, No. 2, 294-301 (1988).
10. D. Banerji and R. Ganguli, Philos. Mag., **13**, No. 6, 494-498 (1932).
11. J. Hay, Can. J. Res., **A16**, No. 1, 191-193 (1938).
12. Kh. A. Dzherpetov and G. M. Patsyuk, Zh. Éksp. Teor. Fiz., **28**, No. 3, 343-351 (1955).
13. S. M. Levitskii, Zh. Teor. Fiz., **27**, No. 5, 1001-1009 (1957).
14. A. A. Kuzovnikov, V. L. Kovalevski, V. P. Savinov, et al., Proc. 13th Conf. Phenom. Ionized Gases, Berlin (1977).
15. A. D. Andreev, Zh. Prikl. Spektrosk., **5**, No. 2, 145-147 (1966).
16. V. A. Golyak, A. A. Kuzovnikov, V. P. Savinov, et al., Vestn. Mosk. Gos. Univ., Ser. Fiz., No. 2, 126-127 (1968).
17. V. A. Godyak and A. A. Kuzovnikov, Fiz. Plazmy, **1**, No. 3, 496-503 (1975).
18. H. Beck, Zs. Physik, **97**, No. 2, 355-360 (1935).
19. Yu. P. Raizer, Physics of the Gas Discharge [in Russian], Moscow (1987).
20. N. A. Yatsenko, Zh. Teor. Fiz., **52**, No. 6, 1220-1222 (1982).
21. N. A. Yatsenko, Teplofiz. Vys. Temp., **20**, No. 6, 1044-1051 (1982).
22. V. A. Godyak and O. N. Popov, Zh. Teor. Fiz., **47**, No. 4, 766-771 (1977).
23. A. A. Kuzovnikov and V. P. Savinov, Vestn. Mosk. Gos. Univ., Ser. Fiz., No. 2, 215-223 (1973).
24. N. A. Yatsenko, Rep. All-Union Seminar HF Breakdown of Gases, Tarty (1989), p. 208-209.
25. A. V. Aleksandrov, V. A. Godyak, A. A. Kozovnikov, et al., Proc. 8th Intern. Conf. Phenom. Ionized Gases, Vienna (1967), p. 165.
26. N. A. Yatsenko, 20th Intern. Conf. Phenom. Ionized Gases, Contr. Papers, Vol. 5, Pisa (1991), pp. 1159-1160.
27. J. Townsend and E. Gill, Philos. Mag., **26**, No. 3, 290-308 (1938).

28. D. He, C. J. Baker, and D. R. Hall, *J. Appl. Phys.*, **55**, No. 11, 4120-4122 (1984).
29. N. I. Lipatov, P. P. Pashinin, A. M. Prokhorov, et al., *Tr. IOFAN*, Vol. 17 [in Russian], Moscow (1989), pp. 53-116.
30. A. V. Kalmykov, Yu. Yu. Nezhentsev, A. S. Smirnov, et al., *Zh. Teor. Fiz.*, **59**, No. 9, 93-97 (1989).
31. P. P. Vitruk and N. A. Yatsenko, *Pis'ma Zh. Teor. Fiz.*, **15**, No. 5, 1-5 (1989).
32. N. A. Yatsenko, 14th Intern. Conf. Coherent and Nonlinear Optics, *Tez. Dokl. Vol. 2* [in Russian], Leningrad (1991), pp. 52-53.

THE PHYSICAL BASES OF SPECTROSCOPIC MEASUREMENTS OF ELECTRICAL FIELDS IN A PLASMA

V. P. Gavrilenko

UDC 533.9.08

Consideration is given to the chief spectroscopic methods of measuring electric fields in plasma media. These methods are based on the effects of Stark splitting of spectral lines of hydrogen atoms, and the appearance of forbidden (by parity) components in the emission spectra of helium atoms. An analysis is made of methods of measuring weak electric fields (with intensities from 10 to 100 V/cm) in plasma. The methods are based on the appearance of forbidden components in the spectra of laser-induced fluorescence of diatomic polar molecules and the Stark effect of Rydberg atoms.

The intraplasma electric field (EF) is one of the most important parameters determining the state and physical processes in a plasma. The EF in a plasma may be caused by natural oscillations of the plasma (e.g., of the Langmuir or ion-acoustic types), the penetration into the plasma from external sources of radiation (e.g., laser or microwave), or the presence of a volume charge (e.g., in the cathode layer of a glow discharge). Furthermore, at every point of a plasma there is an EF created by separate ions and electrons. We note also that the EF may be of the Lorentz type $F_L = c^{-1}[\mathbf{v} \times \mathbf{B}]$ in the case when in the plasma, situated in a magnetic field of strength \mathbf{B} , an atomic beam is injected with velocity \mathbf{v} (for the purpose of heating or diagnostics of the plasma). At the present time, for EF measurements in a plasma, wide use is made of spectroscopic methods based on the Stark effect of atoms, ions and molecules in the plasma. These methods are generally divided into the following groups.

1. Methods of Measuring the EF from the Spectra of Hydrogen Atoms. Since atoms of hydrogen (or deuterium) possess, in their excited states, constant dipole moments, their spectra are very sensitive to the effect of the EF. At the present time, after thorough investigation, wide use is being made in plasma diagnostics of the Stark splitting effect and broadening of spectral lines (SL) of hydrogen atoms in quasistatic (QS) intraplasma EF F . In recent work [1], from the magnitude of the Stark splitting of hydrogen SL, taking into the fine structure of atomic levels, the EF has been measured in the cathode layer of a glow discharge in hydrogen. In [2], from the QS broadening of H_α and H_β SL, a low-frequency anisotropic turbulence has been found in the cathode region of a glow discharge at atmospheric pressure in helium. For measuring the quasimonochromatic linearly polarized EF of the form $E_{lin}(t) = E_0 \cos(\omega t + \varphi)$, use is made of the appearance of satellites in the emission spectrum of atomic hydrogen, which stand apart from the undisplaced position of the hydrogen SL by frequencies $\Delta\omega = \pm p\omega$ ($p = 1, 2, 3, \dots$). The reason for the appearance of the satellites at frequencies $\Delta\omega = \pm p\omega$ (see [3]) is that in a field $E_{lin}(t)$, the hydrogen atom wave function in the α state is described by the expression $\exp[-i(\mathbf{d}_{\alpha\alpha} \cdot \mathbf{E}_0/\omega) \sin(\omega t + \varphi)]$, where $\mathbf{d}_{\alpha\alpha}$ is the dipole moment of the atom in the α state. The appearance of satellites of the hydrogen SL from the effect of a field $E_{lin}(t)$ was first used in [4] for measuring UHF